A Novel Monofilar-Archimedean Metamaterial Inspired Leaky-Wave Antenna for Scanning Application for Passive Radar Systems

Mohammad Alibakhshikenari [1]*, Bal S. Virdee [2], Abdul Ali [1], and Ernesto Limiti [1]

[1] Electronics Engineering Department, University of Rome "Tor Vergata", Via del Politecnico 1, 00133, Rome – ITALY

[2] London Metropolitan University, Center for Communications Technology, School of Computing & Digital Media, London N7 8DB, UK

* alibakhshikenari@ing.uniroma2.it

***Abstract*— A novel backfire-to-endfire leaky-wave antenna is presented with ability to scan from -25° to +45°. The antenna is based on metamaterial transmission-lines (MTM-TLs) and is implemented using Monofilar Archimedean spiral and rectangular slots, spiral inductors and metallic via-holes. The slots act as series left-handed capacitances, and the spirals with via-holes provide the shunt left-handed inductances to realize the metamaterial antenna. A prototype antenna was fabricated prototype on FR4 dielectric substrate, which has an electrical size of $0.0302\lambda_0 \times 0.0357\lambda_0 \times 0.0008\lambda_0$, where λ_0 is free space wavelength at 165 MHz. Measured bandwidth of the antenna is 710 MHz (165-875 MHz) corresponding to a fractional bandwidth of 136.5%. The main advantage of the antenna is its ability to scan over a wide angle from -25° to +45° with acceptable gain and radiation efficiency of 1.2 dBi and 50.1%, respectively, measured at 400 MHz. The wide scanning attributes of the antenna make it suitable for passive radar applications to scan across the VHF-UHF bands for FM-Radio, television, mobile phones and GPS applications.**

Keywords— Leaky-wave antenna; scanning antenna; metamaterial transmission lines; monofilar Archimedean spiral slot.

I. INTRODUCTION

Leaky-wave antennas (LWA) were first proposed for the synthesis of radiation patterns with an optimized main beam covering a specified angular region [1]. Selective radiation beam from this type of antenna is becoming of particular interest for various applications including passive radars and indoor WLAN. Leaky-wave antennas have been used for a long time both in periodic and non-periodic configurations [2]-[4]. However, with the advent of metamaterials [5],[6] novel types of leaky-wave structures have been proposed with average lattice constant or periodicity much smaller than the operating wavelength. Backfire-to-endfire fundamental mode LWA reported in [7]-[9] are based on a novel transmission line approach of realizing composite right/left-handed (CRLH) structures [10]-[13]. Monofilar Archimedean spiral resonator for metamaterial applications was first introduced and modeled by Isik and Esselle in [14].

In this paper we have employed variants of Monofilar Archimedean metamaterial based unit-cells comprising spiral and rectangular configurations in the realization of a novel leaky-wave antenna. The proposed antenna enables scanning over a very wide angle from -25° to +45° which is required by passive antennas that are used to detect and track objects by processing reflections from non-cooperative sources. The proposed LWA design is based on CRLH radiating structure that is composed of: (i) Monofilar Archimedean spiral and rectangular slots that behave as series left-handed (LH) capacitances, and (ii) grounded spiral inductors that behave as shunt LH inductances [15]-[19]. The fringe capacitance and inductance associated with the radiating structure account for the right-handed effects described in [20], which results in a CRLH antenna structure. The proposed metamaterial/CRLH antenna structure exhibits: (i) wide beam steering angle from -25° to 45° compared to [2] which is limited to between -30° to +15°; (ii) has significantly smaller electrical dimensions of $0.0302\lambda_0 \times 0.0357\lambda_0 \times 0.0008\lambda_0$, where λ_0 is free-space wavelength at 165 MHz compared to [2] that has an electrical size of $0.059\lambda_0 \times 0.047\lambda_0 \times 0.004\lambda_0$, where λ_0 is free space wavelength at 930 MHz; and (iii) has a large impedance bandwidth of 136% compared to [2] whose bandwidth is limited to 119%.

II. MTM-BASED LEAKY-WAVE ANTENNA

Geometry of the proposed antenna structure, in Fig.1, shows a radiation patch on which are etched a series of Monofilar Archimedean spiral slots (MASS) and Monofilar Archimedean rectangular slots (MARS). These slots essentially perform the role of series LH capacitors. A mixture of circular and square spiral slots are employed to facilitate coupling moderation between adjacent slots. Lower end of the patch is connected to three conductive spirals that are short-circuited through metallic via-holes, to provide shunt LH inductance. Due to fringe capacitance and inductance associated with microstrip transmission-lines the realization of a purely LH structure is not possible. The antenna is constituted from three unit-cells, where each unit-cell comprises three spiral slots and a grounded inductive spiral. This structure was constructed on FR4 substrate with dielectric constant of 4.3, thickness of 1.6 mm and loss tangent of 0.02. It will be shown that the dimensions of spirals and number of spiral turns have major influence on the performance of the antenna in terms of impedance bandwidth and radiation characteristics. However, it should be noted that there was negligible effect observed on the antenna's performance in the spin direction (i.e. clockwise or anticlockwise) of the rectangular and spiral slits.

Archimedean spiral is defined by [14]:

$$r(\theta)=A\theta^{1/n} \qquad (1)$$

where A and n are real numbers, and θ is the polar angle, which in the proposed design varies over three intervals, i.e. $[\emptyset_1,\emptyset_2]$, $[\emptyset_3,\emptyset_4]$ and $[\emptyset_5,\emptyset_6]$. Spiral and rectangular slots, and the grounded spiral inductor (SI) have a width (w) and a thickness (t), as indicated in Fig. 2. The optimized antenna structure is composed of six MASS, three MARS and three SI. Total shunt inductances (L_L) of the three grounded spirals is:

$$L_L = L_{L_1} + L_{L_2} + L_{L_3} \xrightarrow{L_{L_1}=L_{L_2}=L_{L_3}\ \overrightarrow{yields}} 3L_{L_1} \qquad (2)$$

$$L_{L_1} = \frac{\mu_0 d_{avg}}{2}\left[\ln\left(\frac{d_{avg}}{w}\right) + 0.9 + 0.2\left(\frac{w}{d_{avg}}\right)^2\right] \qquad (3)$$

Where μ_0 is the permeability of free space, and $w = w_{SI} = w_1$, and d_{avg} is the average diameter of the spirals defined by [14]:

$$d_{avg} = \frac{S(\emptyset_5) - S(\emptyset_6)}{\pi\, NT_{SI}} \qquad (4)$$

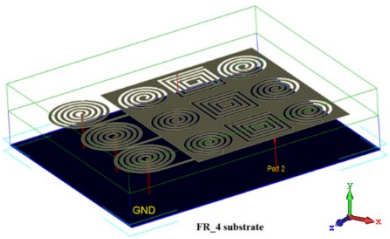

(a) Isometric View

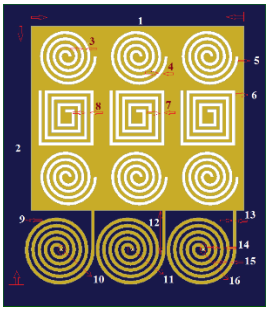

(b) Top View (c) Fabricated Prototype

Fig. 1. Proposed leaky-wave antenna configuration. (Please note, L, W, s_{MASS}, w_{MASS}, NT_{MASS}, NT_{MARS}, w_{MARS}, s_{MARS}, NT_{SI}, D_{via}, w_{via}, L_1, w_1, w_{SI}, s_{SI}, h_{via} are numbered in sequence thus 1, 2, …, 15, 16, respectively.)

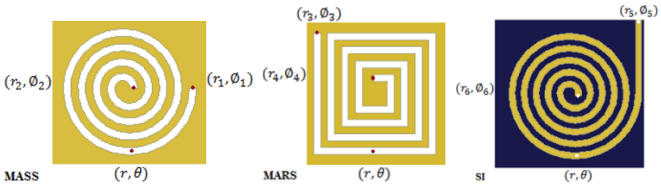

(a) (b) (c)

Fig. 2. Layout of (a) Monofilar Archimedean spiral slot (MASS), (b) Monofilar Archimedean rectangular slot (MARS), and (c) spiral inductor (SI). All three have been constructed using a conductor strip with width w and thickness t.

Spiral arc length is a function of θ and is given by [14]:

$$S(\theta) = A\theta^{1/n}\, {}_2F_6(-1/2, 1/2n;\ 1 + 1/2n\ ;\ -n^2\theta^2) \qquad (5)$$

$$NT_{SI} = (\emptyset_5 - \emptyset_6)/2\pi \qquad (6)$$

Where ${}_2F_6(a, b; c; d)$ represents the hypergeometric function, and NT_{SI} is the number of turns. We have simplified the analysis by ignoring the electromagnetic coupling in the spiral turns.

The self-capacitance of each spiral (MASS) and rectangular (MARS) slot is a combination of the capacitance between the adjacent turns (C_a), and the capacitance between the nearest non-adjacent turns (C_{na}). Total capacitance of the slots is:

$$C_L = \sum_{i=1}^{9} C_{L_i} \xrightarrow[C_{L_2}=C_{L_5}=C_{L_8}]{C_{L_1}=C_{L_3}=C_{L_4}=C_{L_6}=C_{L_7}=C_{L_9}\ \ yields} 6C_{L_1} + 3C_{L_2} \qquad (7)$$

$$C_{L_1} = C_{a_1} + C_{na_1} \qquad (8) \qquad C_{L_2} = C_{a_2} + C_{na_2} \qquad (9)$$

The capacitance between the adjacent turns of spiral and rectangular slots (C_{a_n}) can be approximated by the coplanar strip line (CPS) capacitance per unit length given by [14],[17]:

$$C_{a_1} = l_{gap_1}\, C_{0_1}\, \varepsilon_{eff} \qquad (10) \qquad C_{a_2} = l_{gap_2}\, C_{0_2}\, \varepsilon_{eff} \qquad (11)$$

Where l_{gap_n} is the length of the gap between the adjacent turns which can be calculated using:

$$l_{gap_1} = \frac{[S(\emptyset_1) - S(\emptyset_2 + 2\pi)] + [S(\emptyset_1 - 2\pi) - S(\emptyset_2)]}{2} \qquad (12)$$

$$l_{gap_2} = \frac{[S(\emptyset_3) - S(\emptyset_4 + 2\pi)] + [S(\emptyset_3 - 2\pi) - S(\emptyset_4)]}{2} \qquad (13)$$

C_{0_n} is the capacitance per unit length in the absence of any dielectric substrate, which is given by:

$$C_{0_1} = \varepsilon_0 \frac{K(k_1)}{K(k_1')} \qquad (14) \qquad C_{0_2} = \varepsilon_0 \frac{K(k_2)}{K(k_2')} \qquad (15)$$

Where ε_0 is the permittivity of free space, and K is the complete elliptic integral of the first kind have the following arguments:

$$k_1 = \sqrt{1 - (k_1')^2} \qquad (16) \qquad k_2 = \sqrt{1 - (k_2')^2} \qquad (17)$$

$$k_1' = \frac{s_1}{s_1 + 2\, w_1} \qquad (18) \qquad k_2' = \frac{s_2}{s_2 + 2\, w_2} \qquad (19)$$

Where

$$s_1 = [r(\emptyset_1) - r(\emptyset_2)]/NT_1 - w_1 \qquad (20)$$

$$s_2 = [r(\emptyset_3) - r(\emptyset_4)]/NT_2 - w_2 \qquad (21)$$

Average separation between the spiral and rectangular slot turns are represented by s_1 and s_2, respectively. Widths and number of turns of the spiral slots and spiral conductive strips are represented by w_1, w_2, and NT_1, NT_2, respectively.

In (10) and (11), ε_{eff} is the effective dielectric constant of the coplanar strip line CPS that is a function of the FR4 substrate, the spiral and rectangular configurations. The general formula for ε_{eff} is given as [14]:

$$\varepsilon_{eff} = 1 + \frac{1}{2}\left(\frac{K(k_1)}{K(k_1')}\right) + \frac{1}{2}\left(\frac{K(k_2)}{K(k_2')}\right)\left((\varepsilon_r - 1)\frac{G(g_1')}{G(g_1)}\frac{G(g_2')}{G(g_2)}\right) \qquad (22)$$

Where

$$g_n = \sqrt{1 - (g_n')^2} \qquad (23)$$

$$g_n' = \frac{\sinh(\pi\, s_n/4h)}{\sinh(\pi(s_n + 2w_n)/4h)} \qquad (24)$$

For a thinner dielectric substrate, the effective dielectric constant reduces to:

$$\varepsilon_{eff} = (1 + \varepsilon_r)/2 + (1 - \varepsilon_r)/2 \qquad (25)$$

The capacitance (C_{na}) between the nearest non-adjacent turns of the spiral slits and rectangular slits can be calculated from (10) to (25), but with two modifications. First, by replacing l_{gap} with:

$$l_{gap_1}^{na} = S(\emptyset_1 - 2\pi) - S(\emptyset_2 + 2\pi) \qquad (26)$$

$$l_{gap_2}^{na} = S(\emptyset_3 - 2\pi) - S(\emptyset_4 + 2\pi) \qquad (27)$$

Second, by replacing s with:

$$s_1^{na} = 2[r(\emptyset_1) - r(\emptyset_2)]/NT_1 - w_1 \qquad (28)$$

$$s_2^{na} = 2[r(\emptyset_3) - r(\emptyset_4)]/NT_2 - w_2 \qquad (29)$$

Which represent the average separation between the nearest non-adjacent turns of spiral and rectangular slits, respectively.

Table I shows the extracted parameters using the above equations and following two expressions:

$$L_R = 1/4C_L(\pi\, f_{r_{se}})^2 \quad (30) \qquad C_R = 1/4L_L(\pi\, f_{r_{sh}})^2 \quad (31)$$

Where $f_{r_{se}}$ and $f_{r_{sh}}$ are series and shunt resonance frequencies, respectively. Since, the proposed antenna design is operated under balanced condition, the following applies: $f_{r_{se}} = f_{r_{sh}} = f_r$. Hence, (30) and (31) simplify to;

$$L_R \xrightarrow{balance\ condition} \frac{1}{4C_L(\pi\, f_r)^2} \quad (32)$$

$$C_R \xrightarrow{balanced\ condition} \frac{1}{4L_L(\pi\, f_r)^2} \quad (33)$$

Antenna in Fig. 1 is a two port structure, where port 1 is used to excite the antenna, and port 2 is terminated in a matched 50Ω load. The HFSS EM solver was used to obtain the series ($f_{r_{se}}$) and shunt ($f_{r_{sh}}$) resonance frequencies and the physical parameters of the optimized MTM antenna structure ($d_{avg}, NT_{SI}, s_2, w_1, w_2, NT_1, NT_2\ l_{gap_1}^{na}, l_{gap_2}^{na}, s_1^{na}, s_2^{na}$). This information was then used to determine the equivalent electrical circuit model of the antenna, shown in Fig. 3, which was verified using ADS (RF circuit solver). Length, width and height of antenna are 55 mm, 65 mm and 1.6 mm, respectively. Equivalent circuit model of the proposed metamaterial leaky-wave antenna structure is shown in Fig. 3.

Reflection coefficient response of the circuit model, simulated and measured results of the proposed antenna are compared in Fig. 4. Center frequency of the antenna with the full wave EM solver (HFSS) and circuit model are 425 MHz and 435 MHz, respectively. The measured center frequency of the antenna is 500 MHz. Impedance bandwidth for S_{11}<-10 dB using HFSS, circuit model, and measurement are 710 MHz (160-870 MHz), 706 MHz (162-868 MHz), and 710 MHz (165-875 MHz), respectively; and the corresponding fractional bandwidths are 137.9%, 137.1%, and 136.5%, respectively. There is good agreement between these results. The antenna supports VHF and part of UHF for FM radio, television, mobile phones and GPS applications.

Standard anechoic chamber was used to measure the antenna's gain. In the set-up a transmitting horn antenna was located at the focal point of the reflector to convert the spherical waves to plane waves directed towards the antenna under test. Antenna gain was measured using the standard comparative method. Connector losses were taken into account in the measurements. The radiation efficiency was calculated by taking the ratio of the gain to the directivity (i.e. η = G/D). The directivity was determined by measuring the half power beamwidth of the antenna in radians in the H-plane ($HPBW_H$) and in the E-plane ($HPBW_E$). Directivity was then calculated using $D = 10\log_{10}[4\pi/(HPBW_H \times HPBW_E)]$.

The antenna's simulated and measured radiation characteristics (gain and efficiency) at various spot frequencies are given in Table II. Agreement between the simulated and measured results is very good. The measured peak gain and efficiency of the antenna occurred at 400 MHz (broadside direction) are 1.2 dBi and 50.1%, respectively.

TABLE I. STRUCTURAL PARAMETERS OF ANTENNA IN FIG.1 AND EQUIVALENT CIRCUIT MODEL PARAMETERS EXTRACTED FROM FIG. 3. (UNITS ARE IN MILLIMETER, PF, NH, OHM, 1/OHM)

L	W	s_{MASS}	w_{MASS}	NT_{MASS}	NT_{MARS}	w_{MARS}	s_{MARS}	NT_{SI}	D_{via}	w_{via}	l_1	$w_1 = w_2$
55.75	65.53	0.8	0.8	4	4	0.8	0.8	5	0.6	0.8	10	0.8

w_{SI}	s_{SI}	h_{via}	N_{MASS}	N_{MARS}	N_{SI}	C_{L_1}	C_{L_2}	C_{a_1}	C_{a_2}	C_{na_1}	C_{na_2}	l_{gap_1}
0.8	0.8	1.6	6	3	3	2.88	3.36	1.44	1.68	1.44	1.68	0.8

l_{gap_2}	C_{0_1}	C_{0_2}	ε_{eff}	$l_{gap_1}^{na}$	$l_{gap_2}^{na}$	s_1^{na}	s_2^{na}	A	$\emptyset_1$	$\emptyset_2$	$\emptyset_3$	$\emptyset_4$
0.8	1.2	1.4	1.5	0.8	0.8	0.8	0.8	0.095 mm/rad	$6\pi < \emptyset_1 < 12\pi$	$\pi < \emptyset_2 < 4.5\pi$	$6\pi < \emptyset_3 < 12\pi$	$\pi < \emptyset_4 < 4.5\pi$

$\emptyset_5$	$\emptyset_6$	d_{avg}	L_L	C_L	L_R	C_R	R_L	R_R	G_L	G_R	L_{L_1}	T
$6\pi < \emptyset_5 < 12\pi$	$\pi < \emptyset_6 < 4.5\pi$	0.8	17.65	27.36	10.31	6.54	15.25	11.43	13.85	8.85	5.88	0.8

s_1	s_2	h	w
0.8	0.8	1.6	0.8

NT: Number of turns; *L*: Length; *D*: Diameter; *W*: Width; *S*: Spacing; *N*: Number of MASS/MARS/SI.
HFSS electromagnetic solver was used to extract the above parameters, which were then used to determine the equivalent circuit model using ADS.

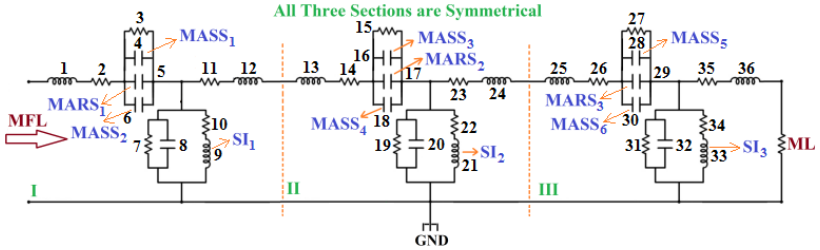

Fig. 3. Equivalent circuit model of the LW antenna based on Monofilar Archimedean spiral, rectangular slits and strips. Numbered in sequence from 1, 2, 3, …, 34, 35, and 36, respectively, are parameters: $\frac{L_{R_1}}{2}$, $\frac{R_{R_1}}{2}$, G_{L_1}, C_{L_1} $(MASS_1)$, C_{L_2} $(MARS_1)$, C_{L_3} $(MASS_2)$, G_{R_1}, C_{R_1}, L_{L_1} (SI_1), R_{L_1}, $\frac{R_{R_1}}{2}$, $\frac{L_{R_1}}{2}$, $\frac{L_{R_2}}{2}$, $\frac{R_{R_2}}{2}$, G_{L_2}, C_{L_4} $(MASS_3)$,

C_{L_5} $(MARS_2)$, C_{L_6} $(MASS_4)$, G_{R_2}, C_{R_2}, L_{L_2} (SI_2), R_{L_2}, $\frac{R_{R_2}}{2}$, $\frac{L_{R_2}}{2}$, $\frac{L_{R_3}}{2}$, $\frac{R_{R_3}}{2}$, G_{L_3}, C_{L_7} $(MASS_5)$, C_{L_8} $(MARS_3)$, C_{L_9} $(MASS_6)$, G_{R_3}, C_{R_3}, L_{L_3} (SI_3), R_{L_3}, $\frac{R_{R_3}}{2}$, and $\frac{L_{R_3}}{2}$. Note, MFL and ML represent the microstrip feed line and matching load, respectively.

Simulated and measured radiation patterns of antenna are shown in Fig. 5. The antenna's radiation extends from -25° (backward radiation) to +45° (forward radiation) with broadside radiation at 0°. The antenna's backward radiation is observed at 165 MHz and 380 MHz, its broadside radiation is observed at 400 MHz, and forward radiations at 450 MHz and 500 MHz. This feature makes the antenna suitable for scanning application necessary for covert passive radar systems.

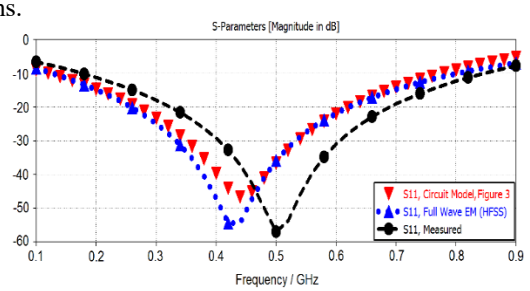

Fig. 4. Simulated and measured reflection coefficient response of the proposed LWA.

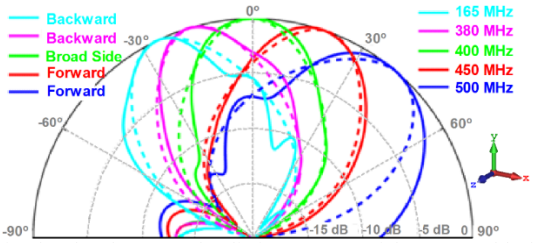

Fig. 5. Simulated and measured radiation patterns of the proposed leaky-wave antenna with scanning capability of -25° (backward radiation) to +45° (forward radiation) with broadside radiation at 0°. Solid lines are with HFSS and dashed lines are with experimental.

III. Conclusions

A new backfire-to-endfire leaky-wave antenna design is shown to be suitable for scanning from -25° to +45° for passive radar applications operating in VHF and UHF bands. The low profile planar antenna has a small footprint and possesses characteristics of wide impedance bandwidth, peak gain (1.2 dBi) and radiation efficiency (50.1%) at 400 MHz. The metamaterial antenna was implemented using Monofilar Archimedean spiral and rectangular slots. The antenna has a measured bandwidth of 710 MHz (165-875 MHz), which corresponds to a fractional bandwidth of 136.5%.

TABLE II. ANTENNA RADIATION SPECIFICATIONS

Frequency (MHz)		165	380	**400**	450	500	875
HFSS™	Gain (dBi)	0.5	1.1	**1.3**	1.0	0.8	0.4
	Efficiency (%)	16.9	43.2	**57.1**	34.8	24.4	14.9
MEASURED	Gain (dBi)	0.3	0.9	**1.2**	0.9	0.7	0.3
	Efficiency (%)	13.6	37.3	**50.1**	30.4	19.2	11.6

REFERENCES

[1] I. Ohtera, "Diverging/focusing of electromagnetic waves by utilizing the curved leaky-wave structure: application to broad-beam antenna for radiating within specified wide-angle," IEEE Trans. Antennas Propag., vol. 47, no. 9, pp. 1470 –1475, Sep. 1999.

[2] M. Alibakhshi-Kenari, A. Andújar and J. Anguera, "New compact printed leaky-wave antenna with beam steering," Microwave & Optical Tech. Lett., vol. 58, issue 1, Jan. 2016, pp. 215–217.

[3] W. Menzel, "A new-traveling wave antenna in microstrip," Arch. Elektron. Uebertrag. Tech, vol. 33, no. 4, Apr. 1979, pp. 137–140.

[4] D.K. Reynolds, W.S. Lucke, "Corrugated endfire antennas," Proc. Nat. Electronics Conf., vol. 6, Sept. 1950, pp. 16–28.

[5] M. Alibakhshi-Kenari, M. Naser-Moghadasi, R. A. Sadeghzadeh, B. S. Virdee and E. Limiti, "Traveling-Wave Antenna Based on Metamaterial Transmission Line Structure for Use in Multiple Wireless Communication Applications", AEUE Elsevier, Volume 70, Issue 12, December 2016, Pages 1645–1650.

[6] M. Alibakhshi Kenari, "Design and Modeling of New UWB Metamaterial Planar Cavity Antennas with Shrinking of the Physical Size for Modern Transceivers," International Journal of Antennas and Propagation, vol. 2013, Article ID 562538, 12 pages, 2013. doi:10.1155/2013/562538.

[7] C. Caloz, T. Itoh, "Novel microwave devices and structures based on the transmission line approach of meta-materials," IEEE MTT-S Int. Symp. Dig., June 2003, pp. 195–198.

[8] C. Caloz, A. Sanada, T. Itoh, "A novel composite right/left-handed coupled-line directional coupler with arbitrary coupling level and broad bandwidth," IEEE Trans.Microwave Theory Tech., vol. 52, March 2004, pp. 980–992.

[9] A. Sanada, C. Caloz, T. Itoh, "Characteristics of the composite right/left-handed transmission lines," IEEE Microwave Wireless Compon. Lett., vol. 14, Feb. 2004, pp. 68–70.

[10] M. Alibakhshi-Kenari, M. Naser-Moghadasi, R. A. Sadeghzadeh and B. S. Virdee, "Metamaterial-Based Antennas for Integration in UWB Transceivers and Portable Microwave Handsets" International Journal of RF and Microwave Computer-Aided Engineering, Volume 26, Issue 1, January 2016, pages: 88–96.

[11] R. A. Sadeghzadeh, M. Alibakhshi-Kenari and M. Naser-Moghadasi, "UWB Antenna Based on SCRLH-TLs for Portable Wireless Devices", Microwave and Optical Tech. Letters, Volume 58, Issue 1, January 2016, Pages: 69–71.

[12] M. Alibakhshi-Kenari, M. Naser-Moghadasi, R. A. Sadeghzadeh and B. S. Virdee, and E. Limiti, "New Compact Antenna Based on Simplified CRLH-TL for UWB Wireless Communication Systems", International Journal of RF and Microwave Computer-Aided Engineering, Volume 26, Issue 3, March 2016, pages: 217–225.

[13] M. Alibakhshikenari, B. S. Virdee, and E. Limiti, "Compact Single Layer Travelling-Wave Antenna Design Using Metamaterial Transmission-Lines" Radio Science, Accepted manuscript online: 23 November 2017, DOI: 10.1002/2017RS006313.

[14] O. Isik K.P. Esselle, "Design of monofilar and bifilar Archimedean spiral resonators for metamaterial applications," IET Microw. Antennas Propag., vol. 3, iss. 6, 2007, pp. 929–935.

[15] O. Isik, K.P. Esselle, "Backward wave microstrip lines with complementary spiral resonators," IEEE Transaction on Antennas and Propagation, vol. 56, no. 10, 2008, pp. 3173–3178.

[16] O. Isik K.P. Esselle, "Design of monofilar and bifilar Archimedean spiral resonators for metamaterial applications" IET Microw. Antennas Propag., vol. 3, iss. 6, 2007, pp. 929–935.

[17] J.D. Baena, J. Bonache, F. Martin, et al., "Equivalent-circuit models for split-ring resonators and complementary split-ring resonators coupled to planar transmission lines," IEEE Trans. Microw. Theory Tech., vol. 53, issue 4, 2005, pp. 1451–1461.

[18] F. Bilotti, A. Toscano, L. Vegni, "Design of spiral and multiple split-ring resonators for the realization of miniaturized metamaterial samples," IEEE Trans. Antennas Propagat., vol. 55, issue 8, 2007, pp. 2258–2267.

[19] O. Isik, K.P. Esselle, Y. Ge, "Archimedean spiral resonators for super compact metamaterial filter design," Proc. Metamaterials 2007: Int. Congress on Advanced Electromagnetic Materials in Microwaves and Optics, Rome, Italy, Oct. 2007, pp. 111–114.

[20] O. Isik, K.P. Esselle, Y. Ge, "Design of archimedean spiral resonators and bandwidth enhancement in filter applications," Proc. Metamaterials 2008: Int. Congress on Advanced Electromagnetic Materials in Microwaves and Optics, Spain, September 2008, pp. 341–345.